Direct Numerical Simulations of Oscillating Liquid Droplets: a Method to Extract Shape Characteristics

Jonathan Reutzsch*[1], Gautham Varma Raja Kochanattu[2], Matthias Ibach[1], Corine Kieffer-Roth[1], Simona Tonini[2], Gianpietro Elvio Cossali[2], Bernhard Weigand[1]
[1]Institut für Thermodynamik der Luft- und Raumfahrt, Universität Stuttgart (ITLR)
Pfaffenwaldring 31, 70569 Stuttgart, Germany
[2]University of Bergamo, Viale Marconi 5 24044 Dalmine, Italy
*Corresponding author: jonathan.reutzsch@itlr.uni-stuttgart.de

Abstract
Oscillating droplets have been an object of various theoretical studies for more than a century and is one of the classic problems in fluid dynamics. A considerable number of theoretical models have been developed and many numerical simulations were conducted to investigate oscillating drops. However, the interplay between analytics and numerics is still not considered sufficiently and is capable of improvement. Thus, the main idea of this work is to extract data from numerical simulations to obtain an extensive comparison between numerics and the available analytical solutions. We present a method to extract surface coordinates of oscillating droplets from numerical simulations and perform a spectral decomposition into Legendre polynomials, in order to derive the different oscillation modes. Various simulations are performed with deviation of the initial droplet shape as well as varying viscosity. In addition, frequencies of the different modes are investigated and compared to analytical models. The method and the numerical results should serve as a basis to improve analytics and to motivate the development of more detailed oscillation models.

Keywords
Droplet oscillation, direct numerical simulation, analytical methods

Introduction

Although it is an inconspicuous small event, oscillations of droplets play a significant role in our daily life and determine various processes in our environment. From raindrops to other weather phenomena to the dripping bottle edge of a red wine, the interaction between surface tension, momentum and viscosity leads to diverse shapes of droplets and to different oscillation behavior. Thus, droplet oscillation has been part of extensive studies in the last century. Nowadays, it is still part of many research works because an exact knowledge of droplet dynamics is needed for the optimization of various technical processes, for instance, atomization of fuel in rocket engines. In order to develop suitable models to describe droplet behavior and interactions on larger scales, the understanding of single droplet oscillation under different conditions is required.
Lord Rayleigh [1] introduced the first model of droplet oscillation in 1879. His model considered an inviscid liquid drop in vacuum to obtain amplitude and frequencies. The normal-mode technique was used to calculate the frequency of the oscillations, which were referred to as “oscillation modes”. Lamb [2] and Chandrasekhar [3] took the effect of viscous and gravitational forces into consideration. Prosperetti [4] worked on the initial value problem of infinitesimal amplitude oscillations of viscous drops. He showed that a more complicated expression than the before mentioned needs to be considered to explain the process of droplet oscillation.
Foote [5] and Alonso [6] performed some of the first numerical simulations of drop oscillations making use of the marker and cell method. Mashayek and Ashgriz [7] used a finite element method to study the oscillations with and without internal circulations. Later Mashayek [8] showed that the period of oscillation is decreased by evaporation even though the dominant mode of oscillation remains the same as for non-evaporating droplets. Schlottke et. al [9] performed numerical simulations of evaporating, deformed droplets. They investigated droplet oscillation in an instationary three dimensional flow field.
Although on the one hand a lot of analytical studies and on the other hand various numerical simulations have been conducted to investigate oscillating drops in the past, the interplay between both disciplines is still capable of improvement. Thus, the main idea of this work is to extract data from high resolved *direct numerical simulations* (DNS) to obtain an extensive comparison between numerics and the available analytical solutions. Furthermore, the numerical results should serve as a basis to improve existing analytical models, for example for droplet oscillations with higher deviations from the initial droplet shape or with evaporation.
We present a method to extract the drop surface coordinates from the numerical simulations of oscillating droplets and perform a spectral decomposition into Legendre polynomials, hence, extracting the different oscillation modes. The simulations are conducted with the multiphase DNS-code *Free Surface 3D* (FS3D), which is described in more detail in the next section. Furthermore, the implementation of the method into the code is part of this work in order

to achieve an efficient workflow, which is desirable due to the high computational load of DNS. Several simulations of oscillating water droplets at standard conditions are performed, comprising 3D setups with an initial deviation of the droplet shape from a spherical case and a variation of physical properties, for instance viscosity. The different oscillation modes are extracted with the mentioned method. Subsequently, they are compared and investigated with regard to their occurrence, amplitudes, frequencies, damping behavior etc. For small initial deviations the dominant modes are analyzed among others by using FFT and compared to the frequency values extracted from analytical equations of Lamb [2] and Prosperetti [4]. We show that the technique is versatile to all different initializations of the droplets, hence, a powerful tool to capture physical changes and suitable for a detailed comparison and interplay between numerics and analytics. Nevertheless, it is a first step in investigating droplet oscillations in such a manner and the work will be extended for various conditions and setups, like droplets with evaporation, higher initial deviations or non-Newtonian properties.

Fundamentals

The simulations are performed with the multiphase code FS3D. The code is used for DNS in order to solve the incompressible Navier Stokes equations. Thus, no turbulence models are needed. The conservation equations are discretized using a finite volume method and a Marker and Cell (MAC) grid, hence, velocities are stored on the cell faces whereas scalars at the cell centers. FS3D uses the *Volume of Fluid* method (VOF), which was developed by Hirt and Nichols [10]. To gain a successful advection the interface is reconstructed with the *Piecewise Linear Interface Calculation* (PLIC) algorithm [11]. Various phenomena have been investigated with FS3D in the last twenty years. Especially in terms of fluid dynamics, such as droplet deformation [12], droplet impact onto a thin film [13] or droplet collisions [14], the code is well validated.

The flow field is computed by solving the conservation equations for mass and momentum

$$\rho_t + \nabla \cdot (\rho u) = 0, \tag{1}$$

$$(\rho u)_t + \nabla \cdot \big((\rho u) \otimes u\big) = \nabla \cdot (S - Ip) + \rho g + f_\gamma, \tag{2}$$

where ρ is the density, u the velocity vector, S the viscous stress tensor defined as $S = \mu\,[\nabla u + (\nabla u)^T]$ with μ denoting the dynamic viscosity and p the pressure. The gravity and other body forces, for instance surface tension, are represented by g and f_γ, respectively. For the description of surface tension different models are implemented in FS3D, such as the conservative continuous surface stress (CSS) model by Lafaurie et al. [15], the continuum surface force model (CSF) by Brackbill et al. [16], and the balanced force approach by Popinet [17]. We used the latter one in the frame of this study. Furthermore, the energy equation is solved in order to deal with heat transfer or phase change phenomena, which is not considered in the frame of this study. According to the VOF method the additional indicator variable f_1 is introduced, which is defined as

$$f_1 = \begin{cases} 0 & \text{in the continous phase} \\ 0 < f_1 < 1 & \text{at the interface} \\ 1 & \text{in the disperse phase.} \end{cases} \tag{3}$$

In this study, the disperse phase is water and the continuous phase is air. On the basis of the one-field formulation, which is inherent to the VOF method, local variables are defined by the local f_1 value, for example the density is calculated from

$$\rho(x,t) = \rho_g + f_1(x,t)\big(\rho_l - \rho_g\big). \tag{4}$$

FS3D is fully parallelized using MPI and OpenMP, therefore, simulations with high computational effort can be conducted. Heretofore, simulations with up to 8 billion cells have been run successfully. For a detailed description of the code or further information we refer to [18].

Method to extract shape characteristics

In the following, we describe our new method to extract the drop surface coordinates from the numerical simulations of oscillating droplets and perform a spectral decomposition into Legendre polynomials to extract the different oscillation modes.

In a first step, the center of mass of the continuous phase, in this paper obviously the center of the droplet, is determined in FS3D. Based on this we determine its distance to the centroid of the PLIC surfaces in every interfacial cell. Hence, extracting a sufficient number of points to describe the shape of the oscillation and applying the spectral decomposition as followed. Figure 1 shows a representative sketch of the droplet with deviation in shape and the PLIC surfaces on the left side. On the right side the PLIC surfaces with their corresponding centroids are depicted in 2D.

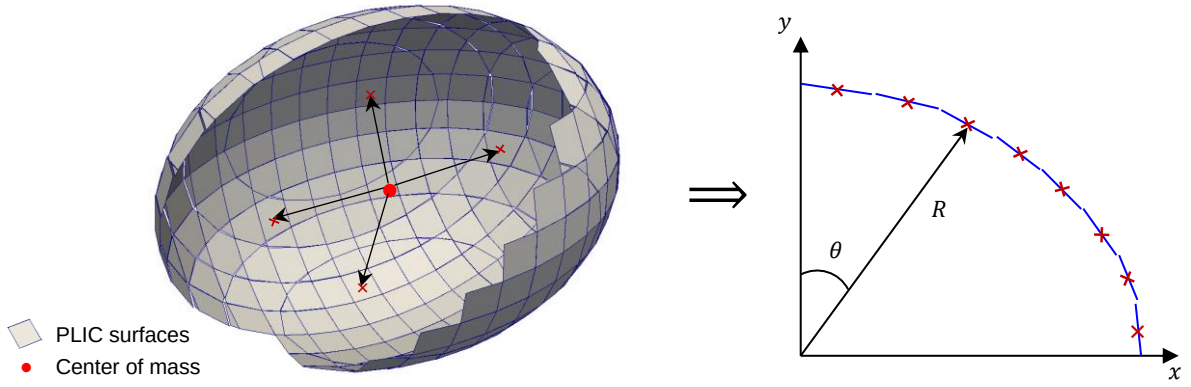

Figure 1. Sketch with PLIC surfaces of a sliced deviated droplet (left). Derived simplified depiction in 2D of FS3D points (right), that are located at the centroids (red crosses) of the PLIC faces.

From every extracted point we derive the radius $R(\eta)$. With the assumption of rotational symmetry we achieve an independency of the azimuthal angle ϕ. Consequently, the radius $R = \sqrt{x^2 + y^2 + z^2}$ is only dependent on the angle $\eta = \cos(\theta) = z/R$. Subsequently, the spectral decomposition of the surface distance can be defined as

$$R(\eta^i) = \sum_{k=0}^{\infty} A_k(t) P_k(\eta^i) \,. \tag{5}$$

$P_k(\eta)$ are the Legendre polynomials of the first kind, k is the number of the mode. In the next section we will show, that in the frame of the regarded setups of this study, odd modes are negligible. Same accounts for modes higher than $k = 6$. The index i represents the total number of points extracted from the simulation, clearly depending on the resolution of the setup. For every time step of the simulation the points are extracted. Equation (5) is then used to fit the solution of the numerical simulation with FS3D by using a least square method according to

$$\sum_{i=1}^{N} \left(R(\eta^i) - R^i_{FS3D}\right)^2 = \sum_{i=1}^{N} \left(\sum_{k=0}^{M} A_k P_k(\eta^i) - R^i_{FS3D} \right)^2 = \mathcal{I} \tag{6}$$

In order to get the best fit between equation (5) and the FS3D radius equation (6) needs to be minimized in terms of each coefficient A_k. Therefore, one obtains

$$\frac{\partial \mathcal{I}}{\partial A_j} = 2 \sum_{i=1}^{N} \left[\left(\sum_{k=0}^{M} A_k P_k(\eta^i) - R^i_{FS3D} \right) P_j(\eta^i) \right] = 0 \tag{7}$$

The values of A_k become a function of time since the form of the droplet changes during its oscillation. Finally, this leads to systems of linear equations in the form

$$\overline{A}_k(t) = \overline{\overline{B}}^{-1}_{kj} \, \overline{T}_j \tag{8}$$

with

$$\overline{\overline{B}}_{kj} = \sum_{i=1}^{N} P_k(\eta^i) P_j(\eta^i) \tag{9}$$

and

$$\overline{T}_j = \sum_{i=1}^{N} R^i_{FS3D} P_j(\eta^i) \,. \tag{10}$$

This procedure for obtaining the values of $A_k(t)$ as a function of time was implemented successfully into FS3D in the frame of this study and will be used in the following to investigate droplet oscillation. First evaluations and results are discussed in the next section.

Results and discussion

The analytical procedure is used to obtain the values of various coefficients $A_k(t)$ and analyze their behavior. For all conducted simulations we use a water droplet at standard conditions and a mass of $m = 2.809237 * 10^{-7}$ kg. The droplet radii of all simulations and the analytics are referred to this mass. Only for the investigations with varying viscosity the material properties obviously differ. All simulations are set up fully 3D with continuous boundaries on all sides of the domain. The droplet is always initialized with the center of mass in the middle of the domain. The distance to the boundaries is chosen in a way that we can insure, that no unintended reactions disturb the oscillation of the droplet.

First, a grid independence study is performed with grid sizes of 32³, 64³, 128³, 256³ and 512³ cells. The droplet is initialized as an ellipsoid with two identical half axes $a = b$ and an initial deviation $\delta = 20\%$ of the third axis c, thus, $c = 1.2a = 1.2b$.

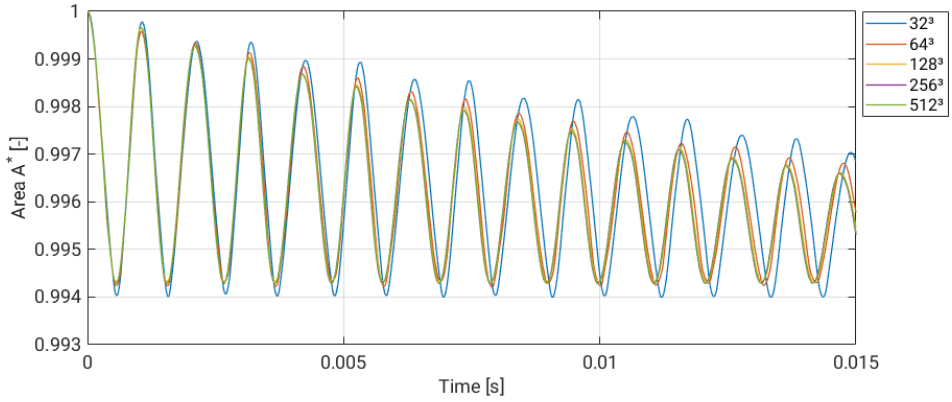

Figure 2. Droplet oscillation for different grid sizes 32³, 64³, 128³, 256³ and 512³. The normalized droplet surface area A^* over time is shown.

Figure 2 shows the normalized area A^* of the droplet surface, which is defined as

$$A^* = A(t)/A(t = 0). \tag{11}$$

When we take the normalized area into consideration, the differences between the various grids is not significant. Even the grid with 32³ cells, which is, as expected, much too coarse for a proper DNS setup, shows a similar behavior at least for the first oscillations. Same accounts for the behavior of the diameter or for the comparison of the three half axes. This shows that simple evaluations, such as complete droplet surface area or diameter, are possible with little computational effort. Previous similar investigations and validations of oscillating droplets with FS3D have already been published by Ertl et al. [19] using a grid of 128³ cells. They proofed this as a sufficient resolution for these simple evaluation characteristic. Figure 2 confirms this assumption, since the devolution of the surface area for grids greater than 128³ cells is almost equal.

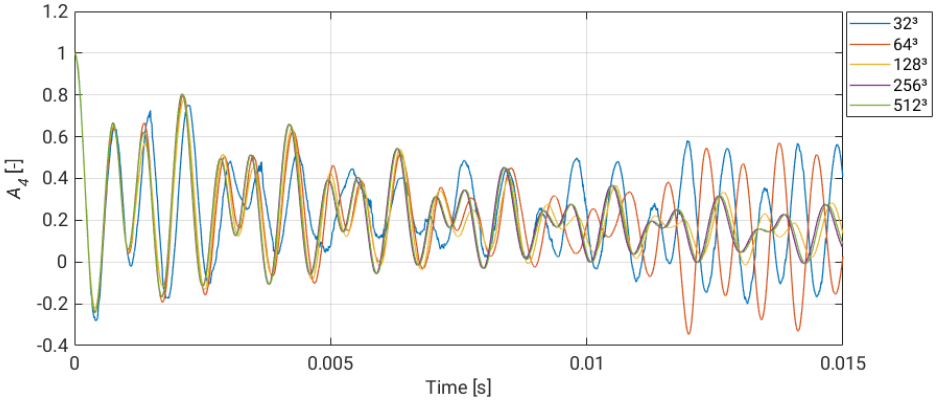

Figure 3. Droplet oscillation with different grid sizes 32³, 64³, 128³ and 256³. The evolution of coefficient A_4 over time is shown.

At this point we will take a look at our new implemented method and examine if the same resolution accounts for the extraction of the different modes. We consider the fourth mode, depicted by A_4 in Figure 3, for exemplary purposes. For the grids coarser than 128³ cells the values partly increase or fluctuate in a non-physical way with ongoing oscillation, presumably due to numerical noise and inaccuracies, inherent to the coarse resolution. However, due to the effect of the viscosity, there must be a damping that exists within the mode which is only depicted by the grids finer than 128³ cells. However, the devolution of the 128³ grid differs with respect to the

amplitudes and frequencies from the finer grid. The difference between the finest grid with 512^3 cells and the 256^3 grid is negligible. Thus, for the following work the 256^3 grid has been utilized, as it provides the best relation between precision and computational costs.

One can clearly see, that for a detailed investigation of a droplet oscillation with a big richness of information, a fine grid is essential. In addition, it is not sufficient to consider simple evaluation techniques, for instance only compare the progression of the diameter over time, when investigating droplet oscillation in such a manner. This is especially true for the development of precise analytical models for predicting droplet behavior or also for investigating smallest initial deviations, like comparing droplets with and without evaporation. The latter will be investigated with the help of our developed method in future studies.

In a next step, we investigate and analyze different oscillating droplets. The following evaluation procedure is applied to all cases. It comprises the devolution of $A_k(t)$, interpretation of their characteristics, identification of numerical noise and an analysis with fast Fourier transform (FFT). Representatively for all cases we choose a water droplet at standard conditions with a small initial deviation of $\delta = 5\%$, which is nominated as *case 1*. The volume, and due to the constant density assumption the mass, is always kept constant for all cases to ensure comparability. In Figure 4 the values of $A_0 - A_{10}$ are plotted over time. A_0 converges to the radius of a volume equivalent sphere, which we nominate as R_0. With the chosen mass of the droplet this leads to a value of about $R_0 \approx 4.06558 * 10^{-4}$ m. This behavior can be seen in all other cases later with ongoing oscillation and damping, independent of the initial deviation. The constant evolution confirms the necessity of a high resolution, since for the coarse grids the value fluctuates much higher. Furthermore, it strengthens the correctness of the implemented method. The values of coefficient A_1 are nearly zero, which is as expected, as it describes the translation of the center of mass. Due to the initialization of a symmetric ellipsoid this point does not move in space. The oscillation of the main mode of the droplet, which is the second mode, represented by A_2, is also clearly visible. Additionally, the damping due to viscosity can be seen with the decreasing of the amplitude of the coefficient A_2 in Figure 4 (left).

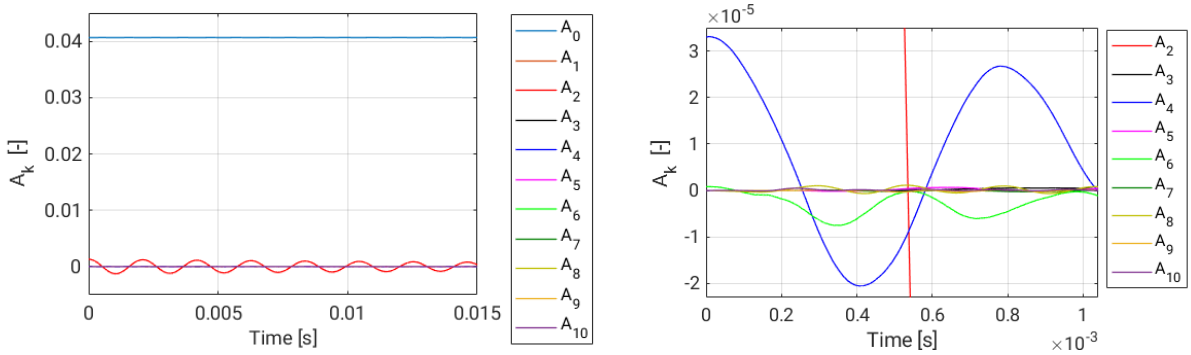

Figure 4. Droplet oscillation of case 1. The complete evolution of all coefficients $A_0 - A_{10}$ over time is shown on the left, a small zoomed part for better visualization on the right. The odd modes are all collapsed on the x-axis.

As expected, the other modes are orders of magnitude smaller and collapse on the x-axis of Figure 4. A detailed investigation and classification of them will be discussed in the following and a further visual insight is given later when we compare different initial deviations δ. The influence of modes higher than A_6 is very small, at least for our considered setups (Figure 4 right). Due to the ellipsoidal initialization of the droplet, that leads to an axisymmetric oscillation in all three main axis, the odd modes should not exist. This is also correct in our cases. The magnitude of the corresponding $A_{k,odd}$ values is negligibly small and is certainly attributed to numerical noise. Indeed, we will see later, that for very low viscosity, meaning unstable numerical droplet oscillation, these modes are growing.

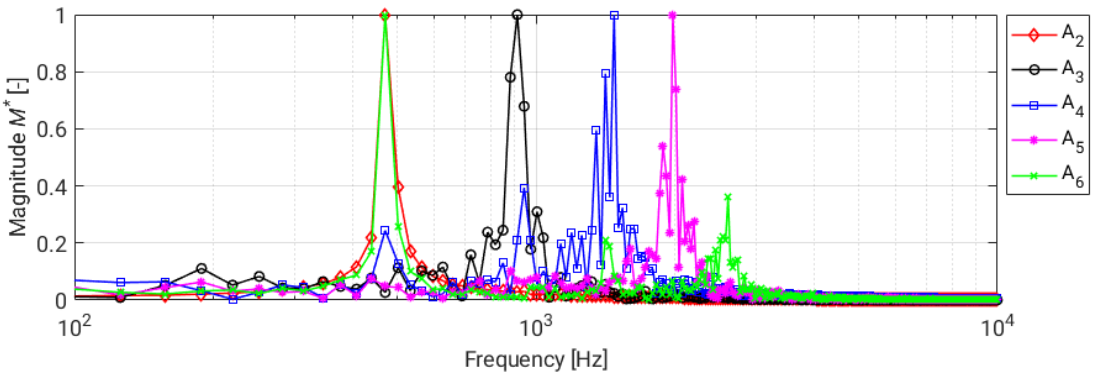

Figure 5. FFT of coefficients $A_2 - A_6$ of case 1.

The different extracted modes are then evaluated using FFT in order to gain the dominant frequencies of the oscillation modes. Figure 5 shows the FFT of the coefficients $A_2 - A_6$ depicted in a semi-logarithmic plot. The normalized magnitude M^* of the FFT is plotted over the logarithmic frequencies. The magnitude is normalized with the maximum occurring value of each coefficient. The corresponding dominant values of the frequencies are given in Table 1. The frequency values for the even modes, in theory the only modes that should be present, show good values, especially the values of A_2 and A_4, which we will show in the following, when comparing to analytical solutions. For the last considered even value of coefficient A_6 one dominant frequency coincides with the one of A_2. This obviously comes from a superposition of both frequencies as well as the very weak signal. Thus, there is probably a numerical influence of the mode A_2 on larger even modes. Nevertheless, the second relevant dominant peak for A_6 is at a frequency of 2608 Hz, which is the expected one.

To validate and verify the values and, thus, our implemented method, we compare case 1 with analytical solutions from Lamb (12) and Prosperetti (13), which read

$$\omega_{Lamb}^2 = \frac{\sigma}{R_0^3 \rho_l} \frac{k(k-1)(k+2)}{\frac{\rho_g}{\rho_l} k + (k+1)} \tag{12}$$

and

$$\omega_{Pros}^2 = k(k-1)(k+2) \frac{\sigma}{(\rho_l R_0^3)}. \tag{13}$$

ω is the angular frequency, σ the surface tension, k as mentioned before the respective oscillation mode. Both analytical solutions are only valid for very small oscillations, thus, a comparison with case 1 is not exact, but appropriate. The frequencies of all modes are, besides the material properties, naturally also depended on the droplet radius. The higher the radius, the lower the frequency of the modes.
The values of the Lamb and Prosperetti frequencies for all considered coefficients $A_2 - A_6$ are also added in Table 1. A comparison with the extracted values from our simulation show, that all are in very good accordance. The deviation for modes $A_2 - A_5$ is less than 1%, the first mode obviously does not exist, and the sixth mode is also proper regarding the mentioned relevant dominant frequency of 2608 Hz. It is noticeable, that the odd modes, which are assumed to be numerical noise, are also in accordance with the analytical solutions obtained from Lamb and Prosperetti.

Table 1. Dominant frequencies obtained from the FFT of coefficients $A_2 - A_6$.

	A_2	A_3	A_4	A_5	A_6
DNS, Dominant frequency [Hz]	471.2	911.1	1421	1979	2608
Lamb frequency [Hz]	468.8	907.8	1407	1961	2568
Prosperetti frequency [Hz]	468.6	907.5	1406	1960	2567
ΔF [%] DNS/Lamb	0.51	0.37	0.99	0.99	1.55
ΔF [%] DNS/ Prosperetti	0.55	0.40	1.07	0.97	1.60

Subsequently, we change the initial deviation δ of the droplet from a sphere to 1%, 20% and 40% and compare the different modes. For the sake of completeness, we add the first case with 5% deviation. The coefficients A_2, A_4 and A_6 over time are depicted in Figure 6. Similar to case 1, the odd modes for the other considered cases have negligible small amplitudes. In order to get a better visible impression of the evolution of the coefficients A_k we look at the first few oscillations. The second mode, which is as mentioned before the main mode, describes the interplay between the different droplet shapes. The oscillation starts with a prolate droplet shape (A_2 positive maximum), reaches the spherical when $A_2 = 0$ and, finally, ends up oblate (A_2 negative maximum). More intriguing than the main mode is obviously the behavior of the fourth mode. One can see clearly, that the coefficient A_4 is predominantly positive. With increasing time and, thus, more damping, its value tends to zero. Especially for high initial deviations it seems to have a growing influence. To understand and evaluate this phenomenon it is worth taking a look inside the literature. Becker et al. [20] investigated large-amplitude oscillations of liquid drops with different initial modes experimentally and theoretically. For the fourth mode oscillation they detected a similar offset of the amplitude from zero. They attributed their observation to a strong nonlinear excitation of higher modes, which cannot be described with linear theory. Hence, also for our elliptical initialization, the extracted fourth mode, and probably the other even modes, seem to follow physical correctness and they are in good accordance with experimental investigations from literature. Noticeable is, that the fluctuations in the curves of the higher modes is probably not a consequence of instabilities or too coarse grid resolution, but of the overlaying of the dominant lower frequency. First investigations with asymmetrical initial droplet shapes support this assumption. Nevertheless, for future investigations, it is indispensable to initialize and evaluate droplets also with the shape of various Legendre polynomials and apply our method to them.

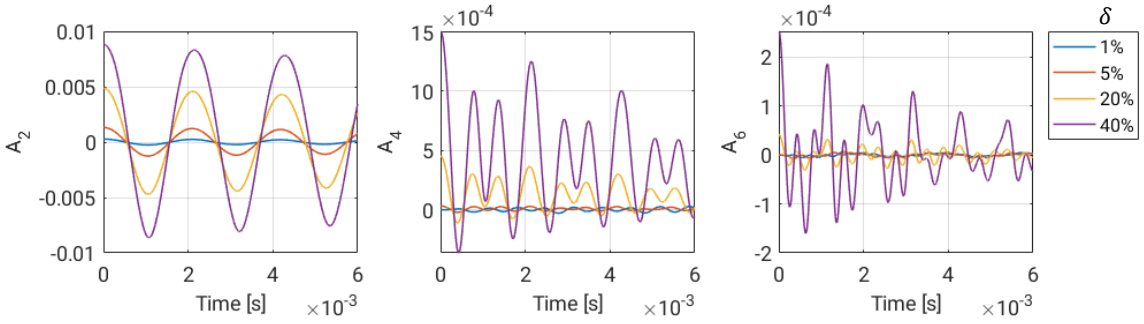

Figure 6. Coefficients A_2, A_4 and A_6 over time of different initial deviations of the droplet.

The evaluation using FFT of the different initial deviations provides no further information. All different main frequencies are of similar magnitude, as expected. Based on the restriction of equal mass of all cases, the shape of the initial ellipsoid naturally varies. Thus, leading to very small differences in the frequency behavior. However, due to the same material properties of all variations, they are negligible. Following this explanation, it makes sense to take a look at the viscosity, which is a determinant factor of droplet oscillation. Hence, in a next step we modify the droplet of case 1 and change its viscosity.

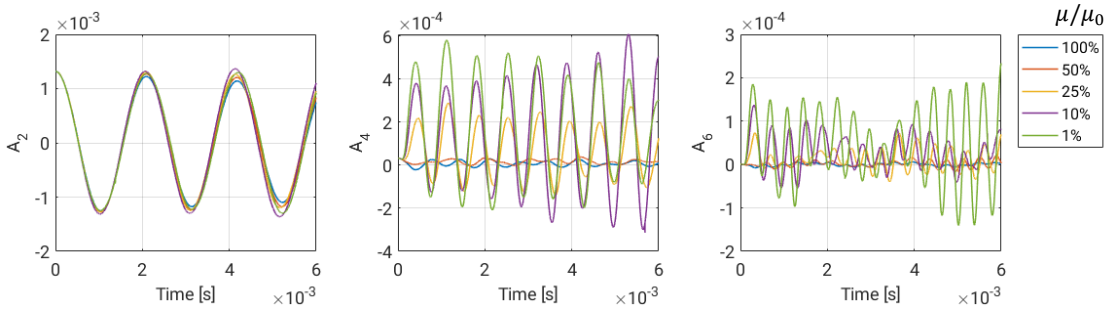

Figure 7. Coefficients A_2, A_4 and A_6 over time of different viscosities of the droplet with an initial deviation of $\delta = 5\%$.

Figure 7 shows the evaluation of the considered even modes over time for different viscosities. Case 1 is referred to the blue line 100%, which is the viscosity for water at standard conditions. Incrementally we change the value from 50% to 1% of this value μ_0. The effect of lower viscosity is clearly visible, as the damping for the main mode is considerably lower. Particularly for 1% and 10% viscosity, the droplet gets very unstable that every mode significantly takes part in the overall oscillations of the droplet. This is the case even for odd modes, which were negligible and, therefore, are not shown in the previous investigation. The FFT analysis also shows chaotic behavior for very low viscosities. During the first oscillations, we yield a higher frequency of the modes, which is of course a consequence of the lower damping. Nevertheless, with proceeding time, we get unstable oscillations and no proper evaluation is possible. The unstable behavior is attributed to spurious numerical effects, which increase apparently with low viscosity, due to the reduced damping effect. The handling of numerical issues, for instance parasitic currents, is a wide field of research and was not a part of this study.

Conclusions

In this paper, oscillation of droplets was investigated. A method has been presented to extract surface coordinates of oscillating droplets from numerical simulations. These coordinates are used to perform a spectral decomposition into Legendre polynomials, in order to extract different oscillation modes. We described the implementation of the method in the multiphase DNS code FS3D. In a first grid study, we demonstrated the necessity of a very high resolution to get satisfying results for the detailed investigation of the modes. Afterwards, several simulations of oscillating water droplets were conducted. We deviated the initial droplet shape and varied viscosity. The modes of these cases were extracted with the help of the described method and analyzed in the following. Furthermore, frequencies of different modes were investigated and compared to analytical models of Lamb and Prosperetti. The results were in very good agreement with the analytical models for small initial deviations. Altogether, the implemented method is able to extract the different modes of various numerical droplet setups. Hence, it is a powerful tool to capture physical changes and it is suitable for a detailed comparison and interplay between numerics and analytics. In the future, the method and the numerical results should serve as a basis to improve and adapt existing analytical models. However, it is a first attempt in evaluating and investigating droplet oscillation. Further studies will be necessary and the works will be extended under various conditions and initializations. These

comprise larger initial deviations, initialization of drops with Legendre polynomials, investigations with evaporating droplets and non-Newtonian material properties.

Acknowledgements

The authors kindly acknowledge the financial support by the Deutsche Forschungsgemeinschaft (DFG) for the International Research Training Group “Droplet Interaction Techmologies” (GRK 2160/1: DROPIT) as well as the Collaborative Research Center SFB-TRR75. In addition, we acknowledge the High Performance Computing Center Stuttgart (HLRS) for support and supply of computational time on the Cray XC40 platform under the Grant No. FS3D/11142.

Nomenclature

A	oscillation mode coefficients [-]
f	VOF variable [-]
g	gravitational acceleration [m s^{-2}]
P	Legendre polynomials [-]
R	radius [m]
u	velocity [m s^{-1}]
p	pressure [N m^{-2}]
δ	deviation [-]
η	angle [rad]
μ	dynamic viscosity [Pa s]
ϕ	azimuthal angle [rad]
ρ	density [kg m^{-3}]
σ	surface tension [N m^{-1}]
θ	polar angle [rad]
ω	angular frequency [s^{-1}]

References

[1] Rayleigh, L., 1879, Proc. R. Soc. London 29.196-199, pp. 71-97.
[2] Lamb, H., 1932, Hydrodynamics, 6th edn, pp. 473-475.
[3] Chandrasekhar, S., 1959, Proceedings of the London Mathematical Society 3.1, pp. 141-149.
[4] Prosperetti, A., 1980, Journal of Fluid Mechanics, 100.2, pp. 333-347.
[5] Foote, G., 1973, Journal of Computational Physics, 11.4, pp. 507-530.
[6] Alonso, C., 1974, "The dynamics of colliding and oscillating drops."
[7] Mashayek, F. and Ashgriz, N., 1998, Physics of Fluids, 10.5, pp. 1071-1082.
[8] Mashayek, F., 2001, International journal of heat and mass transfer, 44.8, pp. 1527-1541.
[9] Schlottke, J., Dulger, E., Weigand, B., 2009, Progress in Computational Fluid Dynamics, 9, no. 6/7.
[10] Hirt, C.W., Nichols, B.D., 1981, Journal of Computational Physics, 39 (1), pp. 201-225.
[11] Rider,W.J., Kothe, D.B., 1998, Journal of Computational Physics, 141 (2), pp. 112-152.
[12] Rieber, M., Graf, F., Hase, M., Roth, N.,Weigand, B., 2000, Proceedings ILASS-Europe, pp. 1-6.
[13] Gomaa, H., Stotz, I., Sievers, M., Lamanna, G., Weigand, B, September 2011, ILASS - Europe, 24th European Conference on Liquid Atomization and Spray Systems.
[14] Roth, N., Gomaa, H., Weigand, B., 2010, Proc. DIPSI Workshop 2010 on Droplet Impact Phenomena & Spray Investigation.
[15] Lafaurie, B., Nardone, C., Scardovelli, R., Zaleski, S., Zanetti, G., 1994, Journal of Computational Physics, 113 (1), pp. 134–147.
[16] Brackbill, J.U., Kothe, D.B., Zemach, C, 1992, Journal of Computational Physics, 100 (2), pp. 335–354.
[17] Popinet, S., 2009, Journal of Computational Physics, 228 (16), pp. 5838–5866.
[18] Eisenschmidt, K., Ertl, M., Gomaa, H., Kieffer-Roth, C., Meister, C., Rauschenberger, P., Reitzle, M., Schlottke, K., Weigand, B., 2016, Journal of Applied Mathematics and Computation, 272 (2), pp. 508–517.
[19] Ertl, M., Roth, N., Brenn, G., Gomaa, H., Weigand, B., September 2013, ILASS - Europe, 25th European Conference on Liquid Atomization and Spray Systems.
[20] Becker, E., Hiller, W. J., Kowalewski, T. A., 1990, Journal of Fluid Mechanics, 231, pp. 180-210.